DOI: 10.1002/chem.200800225

An EXAFS Spectroscopic, Large-Angle X-Ray Scattering, and Crystallographic Study of Hexahydrated, Dimethyl Sulfoxide and Pyridine 1-Oxide Hexasolvated Mercury(II) Ions

Ingmar Persson,*[a] Lars Eriksson,[b] Patric Lindqvist-Reis,[c] Per Persson,[d] and Magnus Sandström[b]

Abstract: The structure of the solvated mercury(II) ion in water and dimethyl sulfoxide has been studied by means of large-angle X-ray scattering (LAXS) and extended X-ray absorption fine structure (EXAFS) techniques. The distribution of the Hg–O distances is unusually wide and asymmetric in both solvents. In aqueous solution, hexahydrated $[Hg(OH_2)_6]^{2+}$ ions in a distorted octahedral configuration, with the centroid of the Hg–O distance at 2.38(1) Å, are surrounded by a diffuse second hydration sphere with $Hg\cdots O_{II}$ distances of 4.20(2) Å. In dimethyl sulfoxide, the six Hg–O and Hg···S distances of the hexasolvated $[Hg\{OS(CH_3)_2\}_6]^{2+}$ complex are centered around 2.38(1) and 3.45(2) Å, respectively. The crystal structure of hexakis(pyridine 1-oxide)mercury(II) perchlorate has been redetermined. The space group $R\bar{3}$ implies six equal Hg–O distances of 2.3416(7) Å for the $[Hg(ONC_5H_5)_6]^{2+}$ complex at 100 K. However, EXAFS studies of this compound, and of the solids hexaaquamercury(II) perchlorate and hexakis(dimethyl sulfoxide)mercury(II) trifluoromethanesulfonate, also with six equidistant Hg–O bonds according to crystallographic results, reveal in all cases strongly asymmetric Hg–O distance distributions. Vibronic coupling of valence states in a so-called pseudo-Jahn–Teller effect probably induces the distorted configurations.

Keywords: dimethyl sulfoxide · hydrates · Jahn–Teller distortion · mercury · structure elucidation

Introduction

Mercury(II) ions often form bonds with a high degree of covalency, which favors low coordination numbers. The configuration of monodentate ligands around mercury(II) is mostly dominated by linear, trigonal, and tetrahedral arrangements; six-coordinated complexes are few and often distorted.[1] The first apparently regular six-coordinated complex was reported for the solid hexakis(pyridine 1-oxide)mercury(II) perchlorate, $[Hg(ONC_5H_5)_6](ClO_4)_2$, with six equidistant Hg–O bonds at 2.35(2) Å, which was determined crystallographically.[2] Subsequently, the crystal structures of other oxygen-donor ligands, that is, hexaaquamercury(II) perchlorate and hexakis(dimethyl sulfoxide)mercury(II) trifluoromethanesulfonate, also displayed solvated mercury(II) ions in sites with six equidistant Hg–O bonds at 2.341(6) and 2.347(5) Å, respectively.[3,4] For hexakis(dimethyl sulfoxide)mercury(II) perchlorate the octahedral coordination is slightly distorted with the two axial Hg–O bonds somewhat longer, $2\times2.376(6)$ Å, than the four equatorial ones, $2\times2.317(6)$ and $2\times2.320(6)$ Å.[5] The tetragonal elongation of the octahedral configuration becomes more pronounced with the somewhat softer electron-pair donor pyridine[6] in hexakis(pyridine)mercury(II) trifluoromethanesulfonate, with the equatorial and axial Hg–N distances within the ranges 2.402–2.442 and 2.497–2.499 Å, respectively.[7] Very

[a] Prof. I. Persson
Department of Chemistry
Swedish University of Agricultural Sciences
P.O. Box 7015, SE-750 07 Uppsala (Sweden)
Fax: (+46) 1867-3476
E-mail: Ingmar.Persson@kemi.slu.se

[b] Dr. L. Eriksson, Prof. M. Sandström
Department of Physical, Inorganic and Structural Chemistry
Stockholm University, SE-106 91 Stockholm (Sweden)

[c] Dr. P. Lindqvist-Reis
Institut für Nukleare Entsorgung, Forschungszentrum Karlsruhe
P.O. Box 3640, D-76021 Karlsruhe (Germany)

[d] Prof. P. Persson
Department of Chemistry, Umeå University
SE-901 87 Umeå (Sweden)

Supporting information for this article is available on the WWW under http://www.chemeurj.org or from the author. It contains crystallographic data in CIF format for **4**, tables of hydrogen atom parameters, anisotropic thermal parameters and least-squares planes.

soft electron-pair donors promote high covalency in the bonds and reduce the coordination number. In liquid ammonia and concentrated aqueous ammonia solutions the mercury(II) ion coordinates four ammonia ligands in a distorted tetrahedral configuration, as well as in the solid state.[8] The mercury(II) ion is four-coordinated in the sulfur-donor solvent *N,N*-dimethylthioformamide, but it was only possible to crystallize a disolvate with linear S–Hg–S coordination.[9,10] Di- and tridentate sulfur-donor ligands are required to form six-coordinated mercury(II) complexes.[11–13] The destabilization of regular six-coordinated mercury(II) complexes, including small monodentate ligands, such as ammonia, is often attributed to a contribution of the mercury(II) $5d_{z^2}$ atomic orbital to the bonding molecular orbitals by vibronic coupling of pseudo-degenerate electronic states in a so-called pseudo-Jahn–Teller effect (PJTE).[14–18] Another explanation for the strong preference for linear two-coordination with a strong covalent contribution by the heavy d^{10} ions mercury(II) and gold(I) has also been suggested: relativistic spin–orbit coupling splits the three 6p orbitals and induces a lower energy for one $6p_{1/2}$ orbital in relation to two degenerate $6p_{3/2}$ orbitals, and the increased closeness of the 6s and 6p valence states thus promotes sp hybridization.[19] However, although relativistic effects certainly contribute to the special properties of the heaviest atoms, this suggestion is not consistent with the similar, albeit weaker, tendency towards the linear two-coordination exhibited by the lighter d^{10} ions silver(I) and copper(I), also with close valence shell states, although no similar tendency of linear coordination is found for cadmium(II).

Theoretical self-consistent field (SCF) calculations of the structures of the hexasolvated divalent ions of Group 12, zinc, cadmium, and mercury, show that the vibronic coupling mode shifts towards lower frequency and increases in amplitude for increasing bond covalency of hexasolvated mercury(II) ions.[18] In addition, the IR spectra display an anomalously broad distribution for the decoupled O–D stretching vibrations of the water molecules in the first hydration sphere around partly deuterated hydrated mercury(II) ions, consistent with dynamic distortions of the Hg–O bonds.[20]

Molecular dynamics simulations with a two-body pair potential for mercury(II) ions in water lead to strongly deviating results, for example, a hydration number of nine. The inclusion of three-body corrections combined with ab initio quantum mechanics/molecular mechanics molecular dynamics (QM/MM-MD) simulations corrected some, but not all, discrepancies, as determined by Kritayakomupong and Rode.[21] Their study using the QM/MM-MD method with three-body correction reported a distorted octahedral first hydration sphere with an average Hg–O distance of 2.42 Å, and a second sphere with 22 water molecules at a mean Hg–O distance of 4.6 Å.[21]

In a recent study that combined X-ray absorption spectroscopic (extended X-ray absorption fine structure (EXAFS) and extended adsorption near edge structure (XANES)) and QM/MD calculations using two-body pair potentials, a flexible seven-coordinated structure with C_2 symmetry was advocated instead of the generally accepted six-coordination.[22] The EXAFS analysis could not distinguish between six-, seven-, or eight-coordination and resulted in an extremely asymmetric distribution of Hg–O distances with a peak maximum at 2.32 Å, independent of the coordination number (CN), and with very large values for the width (σ^2) and asymmetry (C_3) of the bond-distance distribution, 0.025 $Å^2$ and 0.0065 $Å^3$, respectively, for CN = 6 (even somewhat larger for CN = 7 and 8). For six-coordination, our evaluation shows that the reported parameters would correspond to an Hg–O centroid value of 2.46 Å, assuming that the reported Hg–O distance is the peak maximum of the distribution. The QM/MD simulations were interpreted as favoring a seven-hydrated ion, even though the energy differences between six-, seven-, and eight-coordination were very small. XANES calculations were performed and a seven-coordinated configuration with two short Hg–O distances was reported to reproduce the experimental XANES better than regular octahedral or Jahn–Teller-distorted octahedral configurations, in particular, the shoulder on the rising edge in the XANES spectrum. However, we show in this study that similar shoulders appear for all of the studied six-coordinated mercury(II) solvates in the solid state and in solution. This shoulder is especially pronounced for diaquamercury(II) trifluoromethanesulfonate, which has two very short Hg–O distances of 2.11 Å in an almost linear Hg-$(OH_2)_2^{2+}$ entity and four longer distances to the oxygen atoms of the trifluoromethanesulfonate ions at 2.5 Å, which complete the distorted octahedral configuration (see Figure S1 in the Supporting Information).[23]

The structural parameters of the hydrated mercury(II) ion in heavy water were very recently obtained from a neutron-scattering study by using the isotopic substitution technique.[24] The Hg–O and Hg···D distances were found to be 2.48(5) and 3.08(5) Å for 6 ± 1 hydrating water molecules. However, the difference between the diffraction patterns of solutions with different isotopic mercury(II) composition is small and the accuracy of the structural parameters is low.

The distortions induced by the subtle symmetry-reducing PJTE on structures can often more easily be ascertained in solution studies in the absence of competing packing or lattice forces. In this study, six-coordinated mercury(II) complexes in the solid state are found to be distorted even when the configuration appears to be regular. For the corresponding solvated mercury(II) ions in water and dimethyl sulfoxide, the high disorder (Debye–Waller) parameters have previously been found to reflect much larger variations in the bond lengths than is normally found in solvates of divalent metal ions.[25] The high lability of the ligands is also a characteristic feature of the mercury(II) ion, even in complexes with two strong linear Hg–S bonds with thiol groups.[26,27]

Recently, EXAFS studies showed that hexaaquacopper(II) bromate and hexakis(pyridine 1-oxide)copper(II) perchlorate, reported in crystallographic studies to have six equidistant Cu–O bonds in space groups of high symmetry,[28,29] in reality contained Jahn–Teller-distorted, tetragonally elongated CuO_6 octahedra.[30] Hence, in such cases,

when the crystallographic space-group symmetry appears higher than the actual site symmetry of the individual complexes, the results become deceptive. Structural studies should then be complemented with a lattice-independent, structure-sensitive method, such as EXAFS.

Table 1. Solutions studied by LAXS and EXAFS.

Solution	$[Hg^{2+}]$ [mol dm^{-3}]	$[ClO_4^-]$ [mol dm^{-3}]	$[H^+]$ [mol dm^{-3}]	[Solvent]	ρ[a] [g^{-1} cm^{-3}]	μ[b] [cm^{-1}]	Solvent	Method
A	2.00	4.70	0.70	45.32	1.686	50.22	water	LAXS
B	3.041	6.518	0.436	42.67	2.027	75.48	water	LAXS
C	0.911	1.821		13.07	1.385	26.77	Me_2SO	LAXS
D	0.500	1.100	0.100				water	EXAFS
E	0.500	1.000					Me_2SO	EXAFS

[a] Density at ambient temperature. [b] Linear absorption coefficient at ambient temperature for $Mo_{K\alpha}$ radiation.

With this knowledge, the regular Hg–O six-coordination in hexasolvated mercury(II) ions seen in crystal structures was carefully appraised in this study. Hexaaquamercury(II) perchlorate, hexakis(dimethyl sulfoxide)mercury(II) trifluoromethanesulfonate, and hexakis(pyridine 1-oxide)mercury(II) perchlorate all crystallize in high-symmetry space groups, trigonal or hexagonal,[2,4,5] with a site symmetry that would seem to exclude distortions of the complexes. The aims of this study were to evaluate possible dynamic or static structural distortions in oxygen-coordinated solvated mercury(II) ions and to ascertain reliable mean Hg–O distances both in solution and in the solid state, especially for the hydrated mercury(II) ion. Two parallel strategies were employed: 1) solution studies without perturbing lattice effects and 2) structure studies for the solids by the lattice-independent EXAFS method as a complement to crystallographic investigations. The measurements were performed at ambient temperature for the aqueous and dimethyl sulfoxide solutions of mercury(II), at room temperature for the crystalline hexaaquamercury(II) and hexakis(pyridine 1-oxide)mercury(II) perchlorates, and at 298 and 10 K for the hexakis(dimethyl sulfoxide)mercury(II) perchlorate and trifluoromethanesulfonate compounds, respectively. The previous crystallographic study of hexakis(pyridine 1-oxide)mercury(II) perchlorate was undertaken with photographic intensity data at room temperature.[4] This structure has been re-examined at both 100 and 298 K (there is no phase transition between 298 and 100 K); we report only the low-temperature structure herein. The structures of the hydrated and dimethyl sulfoxide solvated mercury(II) ions in solution have also been re-examined with large-angle X-ray scattering (LAXS) and with improved experimental data quality and description of the hydrated perchlorate ion.[31] For the LAXS data, careful modeling of the contribution from the intramolecular O···O distances in the perchlorate ion is essential for reliable evaluation of the Hg–O distance because of their severe overlap.

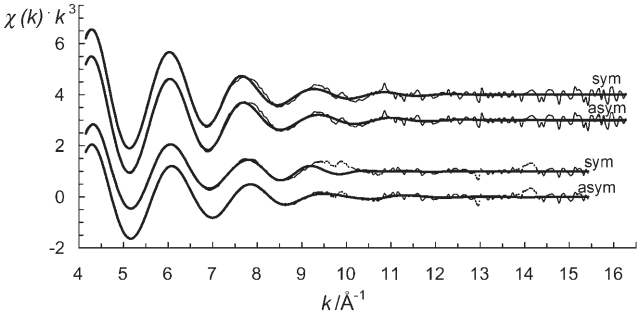

Figure 1. Fit of k^2-weighted EXAFS data for solid $[Hg(H_2O)_6](ClO_4)_2$ (upper) and 0.5 mol dm^{-3} mercury(II) perchlorate in acidic aqueous solution (lower) at room temperature with Gaussian (sym) and asymmetric distributed (asym) Hg–O distances. The dotted regions of the experimental data have been excluded in the refinements.

Results and Discussion

The hydrated mercury(II) ion: The EXAFS oscillations of the hydrated mercury(II) ion show both for the 0.5 mol dm^{-3} solution (D, Table 1) and the hexahydrated perchlorate salt **1** a clear damping of the amplitude and also a significant phase shift at high k values, $k > 9$ Å^{-1} (Figure 1), which indicates a wide and asymmetric distribution of the Hg–O distances.[32] This observation is in contrast with the high amplitude of the EXAFS oscillation at high k values reported by Chillemi et al.[22] (cf. Figure 1), which is probably an artifact caused by the very large and unrealistic C_3 value reported for the model refinement using the program package GNXAS, and/or the presence of a substantial amount of the hydrolysis complex $[Hg(OH)_2]$ with short linear O–Hg–O bonds.[44] The very large C_3 cumulant value causes a very steep slope on the short distance side of the Hg–O distribution, which corresponds to a small disorder (Debye–Waller) parameter and that part of the distribution thereby provides an artificially large contribution to the EXAFS function, in particular at high k values. However, for our two samples, by a careful choice of starting parameters in GNXAS, the EXAFS splines and envelopes became almost identical to those obtained by the program packages EXAFSPAK[33] and WinXAS[34] (the complete data treatment is not presented herein because the results are in very close agreement with those obtained by GNXAS). The data treatment was performed in three different ways:

1) The full EXAFS raw data range was modeled assuming an asymmetric bond distribution (GNXAS), resulting in large, but reasonable, C_3 cumulant parameters (Table 2). The mean Hg–O distance obtained for the hexahydrated ion in the solid compound $[Hg(H_2O)_6](ClO_4)_2$ is $R_c = 2.36(1)$ Å, whereas the peak maximum appears at $R_m = 2.33(1)$ Å. The corresponding values in solution are $R_c =$

Table 2. Mean (centroid) bond lengths (d), the maximum of the radial distribution (R_m) for an asymmetric distribution of bond lengths, disorder parameters ($\sigma = \sqrt{\sigma^2}$ for EXAFS or $= \sqrt{2b}/2$ for LAXS), the number of distances (N), the third cumulant (C_3) of the solvated mercury(II) ions in solids and in solution as determined crystallographically (C), by EXAFS (E), and by LAXS (L) at room temperature or 10 K.

Solvent	State	Interaction	N	d [Å]	R_m [Å]	σ	C_3 [Å]	Angles[a] [°]	Method	Conditions	F[b]
water	solid	Hg–O	6	2.341(6)					C	$[Hg(OH_2)_6](ClO_4)_2$ at RT[3]	
	solid	Hg–O	6	2.362(3)	2.332(3)	0.139(4)	0.53×10^{-3}	∢O-Hg-O 178.1(2), 89.3(5)	E	$[Hg(OH_2)_6](ClO_4)_2$ at RT[c]	1.93×10^{-9}
	solution	Hg–O	6	2.342(4)		0.082(2)			L	$[Hg(OH_2)_6]^{2+}$ at RT	
		Hg···O_{II}	12	4.198(5)		0.212(2)				$Hg(ClO_4)_2$ (2.0 mol dm^{-3})	
		O_I···O_{II}	2	2.814(18)		0.06(2)					
		O_w···O_w	2	2.866(15)		0.086(11)					
		Cl–O	4	1.434(2)		0.050(4)					
		(Cl–)O···O_w	4	3.047(15)		0.095(23)					
		Cl(–O)···O_w	4	3.693(14)		0.101(9)					
	solution	Hg–O	6	2.339(4)		0.088(2)			L	$[Hg(OH_2)_6]^{2+}$ at RT[c]	
		Hg···O_{II}	12	4.200(14)		0.191(4)				3.0 mol dm^{-3} $Hg(ClO_4)_2$	
		O_I···O_{II}	2	2.871(30)		0.07(3)					
		O_w···O_w	2	2.891(13)		0.092(7)					
		Cl–O	4	1.453(2)		0.043(3)					
		(Cl–)O···O_w	4	3.08(4)		0.10(6)					
		Cl(–O)···O_w	4	3.73(4)		0.14(2)					
	solution	Hg–O	6	2.378(3)	2.328(3)	0.148(4)	1.89×10^{-3}	∢O-Hg-O 179.8(2), 85.5(5)	E	$[Hg(OH_2)_6]^{2+}$ at RT[c]	0.68×10^{-9}
Me_2SO	solid	Hg–O	6	2×(2.317+2.320+2.376)					C	**2** at RT[4]	
		Hg···S	6	2×(3.302+3.404+3.520)							
Me_2SO	solid	Hg–O	6	2.402(2)	2.335(4)	0.139(2)	2.09×10^{-3}	∢O-Hg-O 178.6(2), 87.6(4)	E	**2** at RT[c]	2.11×10^{-7}
		S–O	6	1.546(4)		0.085(3)		∢Hg-O-S 121.6(5)			
Me_2SO	solid	Hg–O	6	2.396(2)	2.325(3)	0.117(2)	1.74×10^{-3}	∢O-Hg-O 178.6(2), 87.6(4)	E	**2** at 10 K	0.97×10^{-7}
		S–O	6	1.540(4)		0.061(3)		∢Hg-O-S 121.4(4)			
Me_2SO	solid	Hg–O	6	2.347(5)					C	**6** at RT[6]	
		Hg···S	6	3.333(10)							
Me_2SO	solid	Hg–O	6	2.353(2)	2.335(3)	0.076(2)	0.156×10^{-3}	∢O-Hg-O 178.6(2), 87.6(4)	E	**6** at RT[c]	4.88×10^{-7}
		S–O	6	1.540(4)		0.061(3)		∢Hg-O-S, 115.0(4)			
Me_2SO	solid	Hg–O	6	2.367(2)	2.334(3)	0.081(2)	0.368×10^{-3}	∢O-Hg-O 178.6(2), 87.6(4)	E	**6** at 10 K	5.40×10^{-7}
		S–O	6	1.540(4)		0.061(3)		∢Hg-O-S, 114.8(4)			
Me_2SO	solution	Hg–O	6	2.348(2)		0.075(1)			L	$[Hg\{OS(CH_3)_2)_6]^{2+}$ at RT	
		Hg···S	6	3.414(6)		0.095(1)					
Me_2SO	solution	Hg–O	6	2.380(2)	2.336(4)	0.107(2)	0.82×10^{-3}	∢O-Hg-O 178.6(2), 87.6(4)	E	$[Hg\{OS(CH_3)_2\}]_6^{2+}$ at RT[c]	3.88×10^{-8}
		S–O	6	1.546(4)		0.085(3)		∢Hg-O-S, 121.6(5)			
C_5H_5NO	solid	Hg–O	6	2.346(4)					C	**4** at RT[d]	
		Hg···N	6	3.137							
C_5H_5NO	solid	Hg–O	6	2.399(4)	2.342(4)	0.249(2)	1.41×10^{-3}	∢O-Hg-O 179.8(2), 86.9(5)	E	**4** at RT[c]	4.78×10^{-8}
		N–O	6	1.334(4)		0.142(4)		∢Hg-O-N, 112.7(5)			

[a] Inner core multiple scattering angles. [b] Mean square error. [c] This work. [d] This work and reference [2].

2.38(1) Å and $R_m = 2.33(1)$ Å. The Debye–Waller coefficients are large, $\sigma^2 = 0.019(1)$ and 0.022(1) Å^2, respectively. The fitting of the model to the EXAFS data is shown in Figure 1, and in Figure S2 of the Supporting Information the separate contributions are displayed. The multiple scattering within the HgO_6 core is very small in solution and cannot be discerned in the solid state. No significant contribution from the Hg···H interactions was found, probably due to the large distribution of the Hg–O bonds, see above.

2) The entire range of raw EXAFS data was fitted with a model in which Gaussian distributions of the distances were assumed (GNXAS and EXAFSPAK). A model describing the Hg–O distances as a single Gaussian distribution resulted in a mean value of 2.34(1) Å with Debye–Waller coefficients similar to those obtained for the asymmetric models. A summary of the refined parameters is given in Table S1 of the Supporting Information.
3) A wide Fourier filter ($r-\Delta r \approx 1$–3 Å) was applied and the back-Fourier-transformed oscillation was analyzed within restricted k ranges by fitting a Gaussian Hg–O distance distribution (EXAFSPAK) to evaluate how the contribution shifts in different k ranges (Figure S3 of the Supporting Information). For low k values, all Hg–O distances contribute significantly to the EXAFS oscillations, whereas a fit in the high k range discriminates against weaker bonds with high Debye–Waller parameters. The mean Hg–O distance contribution to the k range 6–10 Å^{-1}, dominated by the more strongly bound water molecules in the hydrated mercury(II) ion, is 2.31(1) Å, whereas for the k range 2–6 Å^{-1} the contribution corresponds to a mean Hg–O distance of 2.34(1) Å.

The three data treatment procedures are all consistent with a wide distribution of Hg–O distances around a peak maximum at 2.34 Å, which corresponds to a large C_3 asymmetry factor, and with a fraction of short and strong Hg–O bonds with a smaller Debye–Waller factor.

From the LAXS data obtained for the two aqueous mercury(II) perchlorate solutions (A and B, Table 1), the radial distribution functions (RDFs) have three peaks at 1.4, 2.3, and 4.2 Å (see Figures 2 and S3). The peak at 1.4 Å corresponds to the Cl–O bond length of the perchlorate ion. The peak at 2.3 Å has two contributions: the main part is in the first hydration shell from the Hg–O distances, together with a contribution from the intramolecular O···O distance of the tetrahedral perchlorate ion (Figure 3). The peak at 4.2 Å corresponds to the second hydration shell, $Hg\cdots O_{II}$. The shoulder at around 3 Å corresponds to O···O distances within the aqueous bulk, $O_w\cdots O_w$, between the water molecules in the first and second hydration sphere, $O_I\cdots O_{II}$, and to O···O distances between water molecules hydrogen-bonded to perchlorate oxygen atoms. The range of the scattering variable, $s = (4\pi/\lambda)\sin\Theta$ is, for a fixed wavelength (λ) by geometry, restricted to a max value, $s_{max} \approx 16$ Å^{-1}, which corresponds to $k \approx 8$ Å^{-1} in the backscattering for pair interactions in EXAFS. This restriction, and also the overlapping interactions from all pairs of distances in solution, does not allow asymmetric distributions to be introduced. All analyses of the LAXS data are therefore performed with Gaussian distributions of distances. However, for long distances, such as to the second hydration sphere, the contribution to the LAXS intensities makes the LAXS data much more informative than the more highly damped backscattering in the EXAFS measurements.[35]

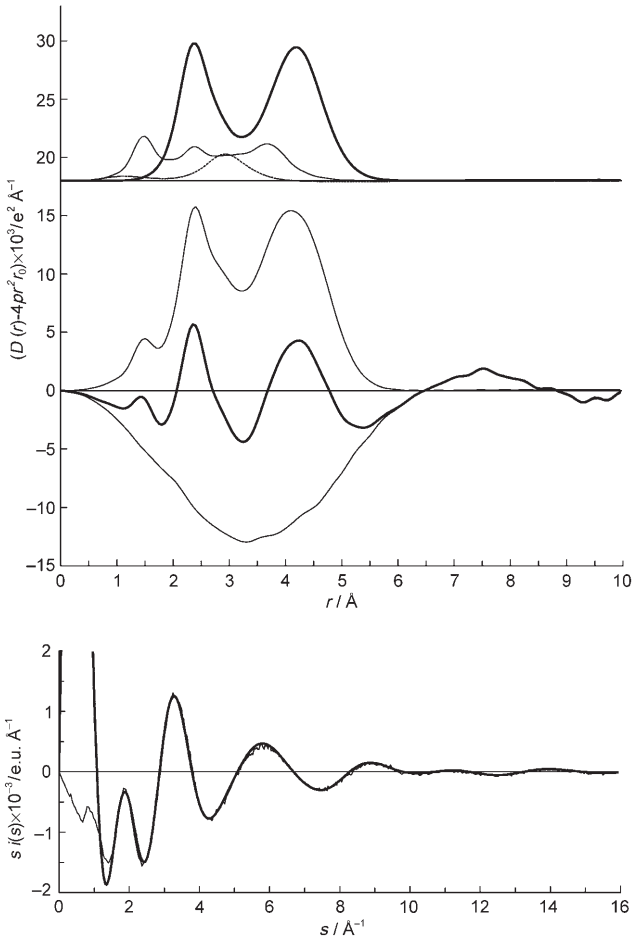

Figure 2. LAXS radial distribution curves for a 3.0 mol dm^{-3} acidic aqueous solution of mercury(II) perchlorate. Top: separate model contributions: the mercury(II) ion with the first and second hydration spheres (——), the hydrated perchlorate ion (——), and hydrogen-bonded $O_w\cdots O_w$ in the aqueous bulk (•••••). Middle: experimental RDF: $D(r)-4\pi r^2\rho_o$ (——), sum of the model contributions (——, upper), and the difference (——, lower). Bottom: structure-dependent LAXS intensity functions: $si_{exp}(s)$ (——) and model $si_{calcd}(s)$ (——).

The Gaussian distributions of the Hg–O distances could for the two LAXS solutions be refined to 2.339(4) and 2.342(4) Å with large displacement factors of $\sigma = 0.082$ and 0.088 Å, respectively; σ is the half-width at half-height of the Gaussian distributed bond length distribution. These values are significantly larger than those normally obtained and imply that the O_I–(H)···O_{II} distribution of the Hg–O bonds in the hydrated mercury(II) ion is at least 0.05 Å wider than that expected for regular octahedral hydrated di-

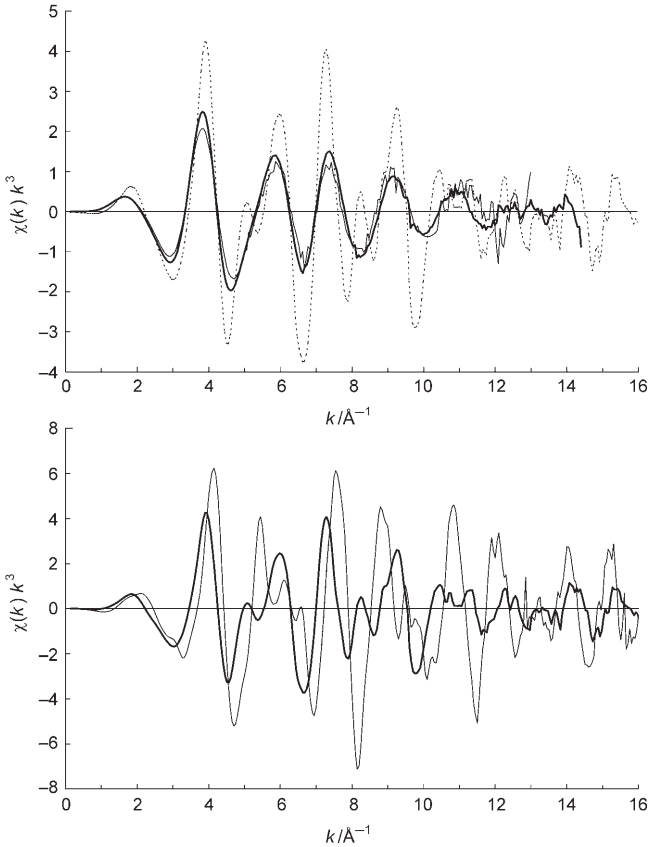

Figure 3. Upper: k^3-weighted raw EXAFS data for solid $[Hg\{OS(CH_3)_2\}_6](ClO_4)_2$ at room temperature (——) and at 10 K (-----), and for 0.5 mol dm^{-3} mercury(II) perchlorate in dimethyl sulfoxide (——) with Gaussian (sym) and asymmetric distributed (asym) Hg–O distances. Lower: k^3-weighted raw EXAFS data for solid $[Hg\{OS(CH_3)_2\}_6](ClO_4)_2$ (——) and $[Hg\{OS(CH_3)_2\}_6](CF_3SO_3)_2$ (——) at 10 K.

valent transition-metal ions.[35] This result is consistent with the EXAFS results and indicates wide and asymmetric distributions of the hydrated mercury(II) ion in both aqueous solution and in the solid state (see above).

A second hydration sphere is clearly indicated with a wide distribution around 4.2 Å (Figure 2), and the mean $Hg\cdots O_{II}$ distance was refined to 4.20(2) and 4.20(1) Å for the 3.0 and 2.0 mol dm^{-3} aqueous solutions, respectively. By assuming 12 water molecules in the second hydration sphere, reasonable values for the disorder parameter (σ) of about 0.2 Å were obtained (Table 2). However, the correlation with the hydration number is strong and the number of water molecules present in the second sphere is uncertain.

The previous infrared absorption difference study of isotopically isolated O–D stretching vibrations resulted in a higher hydrogen-bond strength from the first to the second shell water molecules around the mercury(II) ion than for the hydrated zinc(II) and cadmium(II) ions in aqueous solution, that is, the water molecules bound to the mercury(II) ion are more polarized. Furthermore, the distribution, as estimated from the hydrogen-bond strength of the aqua ligands, is about 0.2 Å broader. The IR study, which was performed for a 0.24 mol dm^{-3} solution of mercury(II) perchlorate, also resulted in about 12 hydrogen-bonded water molecules in the second shell.[20] However, in the concentrated solutions studied in this work, the number of water molecules is not sufficient for an unperturbed second hydration shell (Table 1).

The previous IR study also examined in a similar way the isotopically isolated O–D stretching frequencies of the solid hydrated perchlorates, $[M(OH_2)_6](ClO_4)_2$ (M = Zn, Cd, or Hg).[20] The hydrogen-bond strength of the aqua ligands of the hydrated complexes $[M(OH_2)_6]^{2+}$ was found to be significantly weaker in the solids in which the perchlorate oxygen atoms are acceptors. Otherwise, a similar picture emerged with slightly stronger average hydrogen-bond strengths (average $O_I\cdots O_{II}$ distance estimated to be ≈2.93 Å for mercury, ≈2.96 Å for cadmium) with a wider distribution (≈0.2 Å larger) for the hydrated mercury(II) ion. It was concluded that the pseudo-Jahn–Teller effect affects the Hg–O bonding to a similar extent in the solid structure and in the aqueous solution.[20]

The structure of the hydrated perchlorate ion in the 2.0 mol dm^{-3} mercury(II) perchlorate solution, in which free (bulk) water molecules are present, was found to be identical to that previously reported with a Cl–O bond length of 1.453(2) Å.[31] However, for the 3.0 mol dm^{-3} mercury(II) perchlorate solution, in which stoichiometrically most water molecules are expected to hydrate mercury(II) or be in contact with perchlorate ions, a somewhat shorter Cl–O bond length was obtained, 1.434(2) Å, possibly due to weaker hydrogen bonding in the perturbed water structure.

To summarize, the hydrated mercury(II) ion in aqueous solution is six-coordinated with a broad asymmetric distribution of the Hg–O distances around 2.34(1) Å, a centroid value of 2.38(1) Å, and with a second hydration sphere around 4.20(2) Å. The apparent regular octahedral symmetry of the hexahydrated mercury(II) ions in the solid compound $[Hg(OH_2)_6](ClO_4)_2$ (**1**), as given by the high crystal symmetry in the $P\bar{3}m1$ space group, is evidently an average of randomly oriented PJTE distorted complexes with lower site symmetry, similar to that found for some hexahydrated copper(II) compounds (see the Introduction). However, the structural distortion of the PJTE operating in the hydrated mercury(II) ion is much smaller than the Jahn–Teller distortion described for the hydrated copper(II) ions.[27]

The dimethyl sulfoxide solvated mercury(II) ion: The dimethyl sulfoxide solvated mercury(II) ion in solution (E, Table 1) and in the solid perchlorate compound $[Hg\{OS(CH_3)_2\}_6](ClO_4)_2$ (**2**) revealed large and asymmetric Hg–O distance distributions in the model fitting of the EXAFS data (Table 2). The mean Hg–O distances 2.380(6) and 2.367(6) Å were obtained with somewhat smaller Debye–Waller coefficients than those for the aqueous systems. The analysis of the EXAFS data for **2**, collected at 10 K, gave, within error limits, the same result as the data collected at room temperature (Table 2). The S–O distance has been refined to 1.54(1) Å and the Hg–O–S angle to 121.6(1.2)° for

the mercury(II) ion in dimethyl sulfoxide and to 1.54(1) Å and 121.5(1.0)° for **2**, respectively, at both room temperature and 10 K, which is consistent with the results from the crystallographic determination.[5] The raw EXAFS spectra of **2** at 10 and 298 K, and of the mercury(II) ion in solution are given in Figure 3a.

The EXAFS spectrum of the solid trifluoromethanesulfonate compound $[Hg\{OS(CH_3)_2\}_6](CF_3SO_3)_2$ (**6**) looks somewhat different to that of **2** at 10 K (Figure 3b). Refinement of **6** gave a mean Hg–O distance of 2.353(6) Å. The Debye–Waller coefficient is about 50% smaller than in the solid perchlorate salt (Table 2) with much less asymmetry in the Hg–O bonds. The data collected at 10 K gave an asymmetry twice that found at room temperature, with a mean Hg–O distance of 2.367(6) Å. The S–O distance has been refined to 1.540(8) Å and the Hg–O–S angle 115(1)° for **6** at both room temperature and 10 K, (Table 2) in agreement with the results from the crystallographic determination, 1.542 Å and 116.4°, respectively.[4] The fit of the EXAFS data and the contributions of the individual scattering pathways are shown in Figure S4 of the Supporting Information.

The RDF derived from the LAXS study of the dimethyl sulfoxide mercury(II) perchlorate solution (C) displays three peaks at 1.4, 2.3, and 3.4 Å (see Figure 4). The Cl–O bond length in the perchlorate ion corresponds to the peak at 1.4 Å, and its shoulder to intramolecular distances in the dimethyl sulfoxide molecule. The peaks at 2.3 and 3.4 Å originate from the Hg–O and Hg···S distances, respectively, in the dimethyl sulfoxide solvated mercury(II) ion with a contribution from the O···O distance in the tetrahedral perchlorate ion at 2.33(1) Å. Six Hg–O and Hg···S distances have been refined to 2.348(2) and 3.414(3) Å, respectively, which gives a mean Hg–O–S angle of 122.5°.

The solvated mercury(II) ion in dimethyl sulfoxide and **2** has an asymmetric Hg–O distance distribution similar to that of the hydrated mercury(II) ion. Also the solid trifluoromethanesulfonate compound **6**, in which the six Hg–O bonds appear to be equidistant by crystallography, shows an asymmetric distribution of the Hg–O distances, although they are not as wide as for the corresponding perchlorate salt.

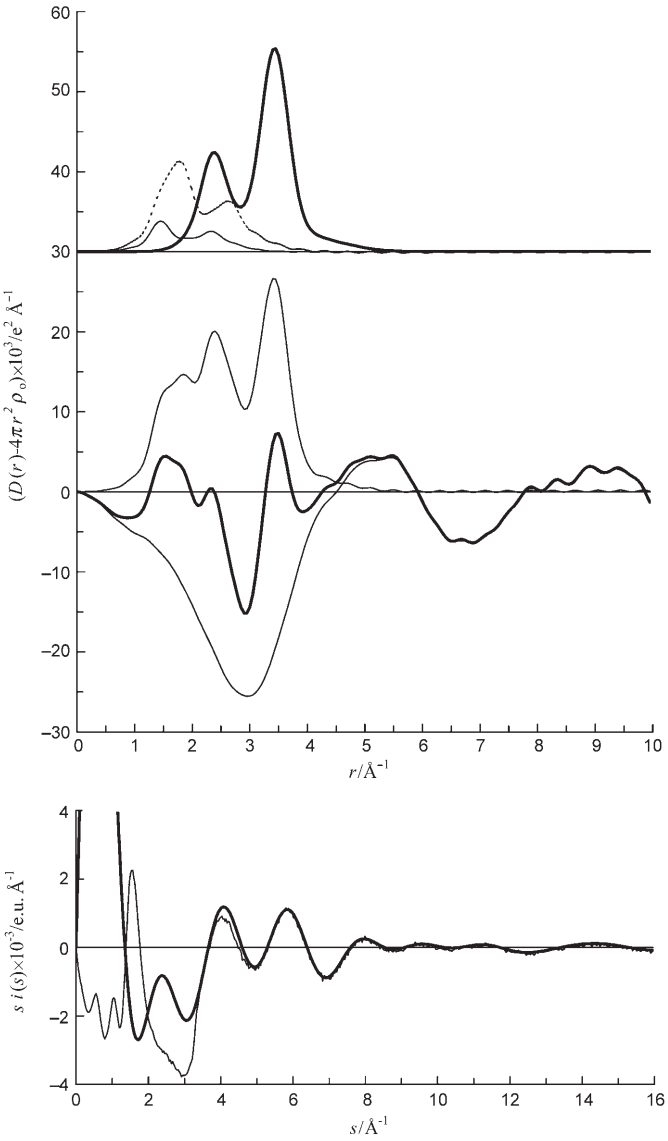

Figure 4. LAXS radial distribution curves for a 1.0 mol dm^{-3} solution of mercury(II) perchlorate in dimethyl sulfoxide. Top: separate model contributions: the dimethyl sulfoxide solvated mercury(II) ion (——), the perchlorate ion (——), and the dimethyl sulfoxide molecule (– – –). Middle: experimental RDF: $D(r)-4\pi r^2\rho_o$ (——), sum of the model contributions (——, upper), and difference (——, lower). Bottom: structure-dependent LAXS intensity functions: $si(s)$ (——) and model $si_{calcd}(s)$ (——).

Structure of hexakis(pyridine 1-oxide)mercury(II) perchlorate (4): The previously reported cell and atomic parameters of **4** have been confirmed with higher precision (see Table 3). Single-crystal X-ray data were obtained at 298 and 100 K and showed that no phase transition occurred within this temperature range; the crystal data obtained at 100 K are given in Table 3. The overall coordination geometry of the hexakis(pyridine 1-oxide)mercury(II) ion can, in accordance with the crystal structure, be described as a near-regular octahedron with S_6 symmetry. The structure shows six equidistant Hg–O distances at 2.3416(7) Å, with *trans* and *cis* O-Hg-O angles of 180.00(4) and 88.79(3)°, respectively. Figure 5 shows the arrangement of the ligands around mercury(II) in the $[Hg(C_5H_5NO)_6]^{2+}$ ion, viewed along the three-fold symmetry axis. No evidence of disordering or large vibrational movements was found for the perchlorate ions in spite of the absence of hydrogen bonds. The perchlorate ion is located on the three-fold axis, with one Cl–O bond along the axis, 1.4366(13) Å, and three equivalent symmetry related Cl–O bonds of 1.4447(9) Å. The average Cl–O distance of 1.442 Å does not vary significantly from the values found in weakly hydrogen-bonded perchlorates, 1.41–1.44 Å, as observed for a large number of compounds.[35]

The N–O distance (1.334 Å) and the mean N–C and C–C distances (1.350 and 1.382 Å) in the pyridine ring differ from those reported in the previous study (1.323, 1.355, and 1.41 Å, respectively).[2] The mean N–O, N–C, and C–C

Table 3. Selected crystallographic data and refinement parameters for **4**.

chemical formula	$[Hg(ONC_5H_5)_6](ClO_4)_2$
empirical formula	$C_{30}H_{30}Cl_2HgN_6O_{14}$
formula weight	970.09
temperature [K]	100
wavelength [Å]	0.71069
crystal system	trigonal/rhombohedral axes
space group	$R\bar{3}$ (No. 148)
unit cell dimensions	
a [Å]	9.6034(4)
α [°]	80.838(4)
volume [Å^3]	855.04(6)
Z	1
ρ_{calcd} [g cm^{-3}]	1.884
μ [cm^{-1}]	47.36
transmission factor	0.63–0.83
crystal size [mm]	$0.10\times0.08\times0.04$
GOF, S	1.091
final R indices [$I>2\sigma(I)$]	
R_1	0.0199[a]
wR_2	0.0362[b]
$\Delta\rho_{min}/\Delta\rho_{max}$ [e Å^{-3}]	−1.592/0.770

[a] $R_1=\Sigma||F_o|-|F_c||/\Sigma|F_o|$. [b] $wR_2=\Sigma[w(F_o^2-F_c^2)^2]/\Sigma(F_o^2)^2$, $S=\Sigma[w(F_o^2-F_c^2)^2]/(n-p)^{0.5}$ $w^{-1}=[\sigma^2(F_o^2)+(0.0180P)^2]$ and $P=(F_o^2)+(2F_c^2)/3$.

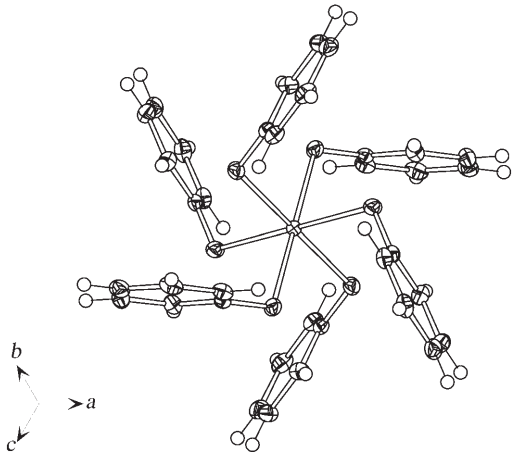

Figure 5. The hexakis(pyridine 1-oxide)mercury(II) ion viewed along the three-fold symmetry axis.

bond lengths in the perchlorate salts of the hexakis(pyridine 1-oxide)zinc(II) and copper(II) complexes (1.324, 1.340, and 1.364 Å, and 1.330, 1.341, and 1.374 Å, respectively[2,26]) agree well with the values obtained for the hexakis(pyridine 1-oxide)mercury(II) complex reported herein (see Table S2 of the Supporting Information). The *trans*-pyridine rings are coplanar and the angle between the *trans*- and *cis*-pyridine ligands is 62.46(4)°.

The fitting of the room-temperature EXAFS data of **4** resulted in a very similar pattern to that found for the PJTE distorted hydrated and dimethyl sulfoxide solvated mercury(II) ions (see above). The refinements gave a mean Hg–O distance of 2.399(6) Å, a peak maximum at 2.342 Å, a large displacement factor of $\sigma=0.125(6)$ Å, and a significant asymmetry of $C_3=0.00141(12)$ Å^3. The Hg–O–N bond angle was refined to 112.7(1.0)°, which is in good agreement with the crystallographic value of 112.21(5)°. The fit of the EXAFS data is given in Figure S5 of the Supporting Information.

Conclusion

The similar wide and asymmetric distributions of distances shown by EXAFS studies for the distorted hexasolvated mercury(II) ions in solid compounds and in the corresponding aqueous and dimethyl sulfoxide solutions show that the mercury(II) ion maintains six-coordination in solution. An appreciably longer mean Hg–O distance would be expected for a seven-coordinated mercury(II) ion, as proposed by Chillemi et al.,[22] compared with that observed for hexasolvated mercury(II) ions in the solid state. In a comparable case, for cadmium(II), the mean Cd–O distance in hexasolvated cadmium complexes in the solid state is significantly shorter than those observed in water and dimethyl sulfoxide, which supports the partial (ca. 35%) presence of a seven-coordinated complex.[36]

The distorted configuration of the six Hg–O distances in solvated mercury(II) complexes in water and dimethyl sulfoxide is consistent with a contribution of the mercury(II) $5d_{z^2}$ atomic orbital to the bonding molecular orbitals in a vibronic PJTE coupling of close-lying electronic states of E_g symmetry. This is also the case for the three crystal structures in which the site symmetry is consistent with six equidistant Hg–O bonds, but for which the EXAFS studies reveal wide and asymmetric Hg–O bond distributions. The XANES regions for all the six-coordinated complexes studied in this work are very similar with a shoulder on the rising edge for all solids and solutions. In particular, the compressed octahedral HgO_6 coordination with a linear entity in the solid dihydrate $[Hg(H_2O)_2(CF_3SO_3)_2]_\infty$ displays a marked peak (Figure S1 of the Supporting Information). When the softness of the ligand and the covalency of the bonds increases, for example, for the sulfur-donor solvent *N,N*-dimethylthioformamide and for liquid ammonia, the amplitude of the vibrational asymmetric stretching frequency increases[18] and evidently promotes a decrease in the coordination number of mercury(II) to distorted tetrahedral complexes, or ultimately, as in the solid state, to linear two-coordination.

Experimental Section

Preparation of solids: Hexaaquamercury(II) perchlorate, $[Hg(OH_2)_6](ClO_4)_2$ (**1**),[3] hexakis(dimethyl sulfoxide)mercury(II) perchlorate, $[Hg\{OS(CH_3)_2\}_6](ClO_4)_2$ (**2**),[5] octakis(dimethyl sulfoxide)dimercury(II) perchlorate, $[Hg_2\{OS(CH_3)_2\}_8](ClO_4)_4$ (**3**),[5a] hexakis(pyridine 1-oxide)mercury(II) perchlorate, $[Hg(ONC_5H_5)_6](ClO_4)_2$ (**4**),[2] anhydrous mercury(II) trifluoromethanesulfonate, $Hg(CF_3SO_3)_2$ (**5**),[37] and hexakis(dimethyl sulfoxide)mercury(II) trifluoromethanesulfonate, $[Hg\{OS(CH_3)_2\}_6](CF_3SO_3)_2$ (**6**),[4] were prepared as described previously.

Preparation of solutions: The aqueous solutions were prepared by dissolving weighed amounts of mercury(II) oxide (Merck) in perchloric acid

(BDH) at 80 °C. The solutions were filtered before analysis. The solutions in dimethyl sulfoxide were prepared by dissolving weighed amounts of **3** in freshly distilled dimethyl sulfoxide. The concentration of mercury(II) was determined by ethylenediaminetetraacetic acid (EDTA) titration;[38] the solutions in dimethyl sulfoxide were diluted with water. The anion concentration in solution was determined by titrating the eluent from a cation exchange resin with a standard sodium hydroxide solution (Table 1). The densities of the solutions were measured with an Anton Paar DMA 35 densitometer.

Crystallography: Data collection for the crystal structure of **4** was carried out with an Xcalibur KM4 diffractometer equipped with a sapphire-III CCD[39] using $Mo_{K\alpha}$ radiation ($\lambda = 0.71073$ Å) at 100 K. Details of the structure determination can be found in Table 3. The structures were solved by direct methods using SHELXS97[40] for which the majority of the non-hydrogen atoms could be found in the initial electron density map. The models were refined by least-squares methods using the SHELXL97[40] program for which the remaining atoms could be found from difference density maps. The hydrogen atoms were positioned geometrically to ride on the parent carbon atoms in the least-squares refinements. All non-hydrogen atoms were refined with anisotropic displacement parameters. Geometrical information was also obtained by using PLATON,[41] and Figure 5 was drawn with DIAMOND.[42]

EXAFS data collection: Mercury L_{III}-edge X-ray absorption data were measured at the Stanford Synchrotron Radiation Laboratory (SSRL) using the wiggler beam line 4-1, which was equipped with a Si[220] double-crystal monochromator. The storage ring was operated at 3.0 GeV and a maximum current of 100 mA. Data collection was performed in transmission mode at ambient temperature, and higher-order harmonics were rejected by detuning the second monochromator crystal to 50 % of maximum intensity at the end of the scans. The solids were diluted with boron nitride to give an approximate edge step of about one unit in the logarithmic intensity ratio. The solutions were kept in cells with 6 μm polyethylene film windows and 1–5 mm Teflon spacers. The X-ray absorption spectra were energy calibrated by means of a simultaneously measured amalgamated tin foil as internal standard; the first inflection point of the mercury metal L_{III}-edge was assigned an energy of 12284 eV.[43] The EXAFSPAK program package was used for averaging 3–5 spectra for each sample after energy calibration.[33]

EXAFS data analysis: For further data treatment two independent software packages were used: GNXAS,[44] with options to model an asymmetric distribution of the Hg–O distances, and EXAFSPAK,[33] with all distances in Gaussian distributions. The EXAFS oscillations were obtained after pre-edge subtraction, normalization, and spline removal.[45] Model refinements in EXAFSPAK use ab initio calculated phase and amplitude parameters obtained from the FEFF7 program for single and multiple scattering pathways.[46] The input files to FEFF7 were compiled from the corresponding crystal structures to contain the Cartesian coordinates of all atoms within a 5 Å radius from the mercury center.

The GNXAS code models the EXAFS signal with subsequent refinement of the structural parameters.[44] The GNXAS method accounts for multiple-scattering (MS) pathways and calculates the configurational average of all the MS signals to allow fitting of correlated distances and bond length variances (Debye–Waller coefficients). A detailed description of the first coordination sphere of any hydrated/solvated metal complex should, in principle, take some asymmetry into account in the distribution of the ion–solvent bond lengths.[47,48] For the distribution of the Hg–O distances, the asymmetry was very pronounced and was modeled in r space with a Γ-like distribution function that depends on four parameters,: the coordination number (N), the average distance (R), the mean-square variation (σ), and the skewness (β). Curve fitting was performed by describing an asymmetric distribution of the Hg–O distances by means of cumulant expansion of the pair-distribution function. The β parameter is related to the third cumulant (C_3) in a cumulant expansion through the relationship $C_3 = \sigma^3\beta$. R is the first moment of the function $4\pi\int g(r)^2 dr$, in which r is the average (centroid) distance and not the position of the maximum of the distribution (R_m).

A special feature of the EXAFS investigations of the solvated mercury(II) ions, both in solution and the solid solvates, is that the rapidly decreasing amplitude of the oscillations makes the splining procedure for background removal especially problematic. The spline refinement employed in the GNXAS program, in which the entire EXAFS spectrum is modeled, turned out to be easy to apply and reliable, provided the starting model is close to the final one.

Large-angle X-ray scattering (LAXS): The scattering of $Mo_{K\alpha}$ X-ray radiation ($\lambda = 0.7107$ Å) from the free surface of aqueous and dimethyl sulfoxide solutions of mercury(II) perchlorate (Table 1) was measured by means of a large-angle Θ-Θ diffractometer at discrete points in the range $1 < \Theta < 65°$; the scattering angle was 2Θ.[20,49] The solutions were contained in a Teflon cup inside an air-tight radiation shield with beryllium windows. The scattered radiation was monochromatized in a focusing LiF crystal monochromator. At each pre-set angle 100000 counts were accumulated and the entire angular range was scanned twice, which corresponds to a statistical error of about 0.3 %. The divergence of the primary X-ray beam was limited by 1, $^1/_4$, or $^1/_{12}°$ slits for different Θ regions, with overlapping data for scaling purposes. The experimental setup and the theory of the data treatment and modeling have been described elsewhere.[10] All of the data treatment was carried out by using the KURVLR program.[50] The experimental intensities were normalized to a stoichiometric unit of volume that contains one mercury atom by using the scattering factors f for neutral atoms, including corrections for anomalous dispersion,[51] $\Delta f'$ and $\Delta f''$, and for Compton scattering.[52] Least-squares refinements of the model parameters were carried out by means of the STEPLR program[53] in which the expression $U = \Sigma[si_{exp}(s) - si_{calcd}(s)]^2$ ($i(s)$ is the reduced intensity and s is the scattering variable, $s = (4\pi/\lambda)\sin\theta$) is minimized and the scattering variable is $s = (4\pi/\lambda)\sin\theta$. The model parameters were refined for data in the high s region, for which the intensity contribution from the long-range distances can be neglected.[54] A Fourier back-transformation procedure was used to improve the alignment of the experimental structure-dependent intensity function $i_{exp}(s)$ before the refinements by removing spurious non-physical peaks below 1.2 Å in the radial distribution function.[49]

Acknowledgements

We gratefully acknowledge the support given to these investigations by the Swedish Research Council. Portions of this research were carried out at the Stanford Synchrotron Radiation Laboratory (SSRL), a national user facility operated by Stanford University on behalf of the U.S. Department of Energy, Office of Basic Energy Sciences. The SSRL Structural Molecular Biology Program is supported by the Department of Energy, Office of Biological and Environmental Research, and the National Institutes of Health National Center for Research Resources, Biomedical Technology Program.

[1] D. Grdenic, *Quart. Rev. Chem. Soc.* **1965**, *19*, 303–328.
[2] D. L. Kepert, D. Taylor, A. H. White, *J. Chem. Soc., Dalton Trans.* **1973**, 670–673.
[3] G. Johansson, M. Sandström, *Acta Chem. Scand., Ser. A* **1978**, *32*, 109–113.
[4] J. M. Hook, P. A. W. Dean, D. C. R. Hockless, *Acta Crystallogr., Sect. C* **1995**, *51*, 1547–1549.
[5] M. Sandström, I. Persson, *Acta Chem. Scand., Ser. A* **1978**, *32*, 95–100.
[6] M. Sandström, I. Persson, P. Persson, *Acta Chem. Scand.* **1990**, *44*, 653–675.
[7] R. Åkesson, M. Sandström, C. I. Stålhandske, I. Persson, *Acta Chem. Scand.* **1991**, *45*, 165–171.
[8] a) P. Nockemann, G. Meyer, *Z. Anorg. Allg. Chem.* **2003**, *629*, 123–128; b) K. B. Nilsson, M. Maliarik, I. Persson, A. Fischer, A.-S. Ullström, M. Sandström, *Inorg. Chem.* **2008**, *47*, 1953–1964.
[9] C. M. V. Stålhandske, C. I. Stålhandske, M. Sandström, I. Persson, *Inorg. Chem.* **1997**, *36*, 3167–3173.

[10] C. M. V. Stålhandske, I. Persson, M. Sandström, E. Kamienska-Piotrowicz, *Inorg. Chem.* **1997**, *36*, 3174–3182.
[11] A. J. Blake, A. J. Holder, T. I. Hyde, G. Reid, M. Schröder, *Polyhedron* **1989**, *8*, 2041–2045.
[12] W. N. Setzer, G. J. Qin Guo, J. L. Hubbard, R. S. Glass, D. G. van Derveer, *Heteroat. Chem.* **1990**, *1*, 375–387.
[13] J. Pickardt, J. Shen, *Z. Naturforsch. B* **1993**, *48*, 969–972.
[14] L. E. Orgel, *J. Chem. Soc.* **1958**, 4186–4190.
[15] R. S. Nyholm, *Proc. Chem. Soc. London* **1961**, 273–320.
[16] I. B. Bersuker, *The Jahn–Teller Effect and Vibronic Interactions in Modern Chemistry*, Plenum Press, New York, **1984**, Chapters 1–5.
[17] I. B. Bersuker, V. Z. Polinger, *Vibronic Interactions in Molecules and Crystals*, Springer, Berlin, **1989**, Chapters 3 and 4.
[18] D. Strömberg, M. Sandström, U. Wahlgren, *Chem. Phys. Lett.* **1990**, *172*, 49–54.
[19] G. Meyer, P. Nockemann, *Z. Anorg. Allg. Chem.* **2003**, *629*, 1447–1461.
[20] P.-Å. Bergström, J. Lindgren, M. Sandström, Y. Zhou, *Inorg. Chem.* **1992**, *31*, 150–152.
[21] C. Kritayakomupong, B. M. Rode *J. Chem. Phys.* **2003**, *118*, 5065–5070.
[22] G. Chillemi, G. Mancini, N. Sanna, V. Barone, S. Della Longa, M. Benfatto, N. V. Pavel, P. D'Angelo, *J. Am. Chem. Soc.* **2007**, *129*, 5430–5436.
[23] A. Molla-Abbassi, L. Eriksson, P. Lindqvist-Reis, J. Mink, I. Persson, M. Sandström, M. Skripkin, A.-S. Ullström, *J. Chem. Soc., Dalton Trans.* **2002**, 4357–4364.
[24] O. Sobolev, G. J. Cuello, G. Román-Ross, N. T. Skipper, L. Charlet, *J. Phys. Chem. A* **2007**, *111*, 5123–5125.
[25] M. Sandström, I. Persson, S. Ahrland, *Acta Chem. Scand. Ser. A* **1978**, *32*, 607–625.
[26] F. Jalilehvand, B. O. Leung, M. Izadifard, E. Damian, *Inorg. Chem.* **2006**, *45*, 66–73.
[27] G. N. George, R. C. Prince, J. Gailer, G. A. Buttigieg, M. B. Denton, H. H. Harris, I. J. Pickering, *Chem. Res. Toxicol.* **2004**, *17*, 999–1006.
[28] A. C. Blackburn, J. C. Gallucci, R. E. Gerkin, *Acta Crystallogr., Sect. C* **1991**, *47*, 2019–2023.
[29] C. J. O'Connor, E. Sinn, R. L. Carlin, *Inorg. Chem.* **1977**, *16*, 3314–3320.
[30] I. Persson, P. Persson, M. Sandström, A.-S. Ullström, *J. Chem. Soc., Dalton Trans.* **2002**, 1256–1265.
[31] P. Lindqvist-Reis, A. Munoz-Paez, S. Diaz-Moreno, S. Pattanaik, I. Persson, M. Sandström, *Inorg. Chem.* **1998**, *37*, 6675–6683.
[32] I. Persson, M. Sandström, H. Yokoyama, M. Chaudhry, *Z. Naturforsch. B Chem. Sci.* **1995**, *50*, 21–37.
[33] G. N. George, I. J. Pickering, EXAFSPAK, A Suite of Computer Programs for EXAFS Analysis, SSRL, Stanford University, Stanford CA (US), **1993**.
[34] T. Ressler, *J. Synchrotron Radiat.* **1998**, *5*, 118–122.
[35] a) The Cambridge Crystallographic Data Centre: computer-based search, retrieval, analysis, and display of information: F. H. Allen, S. Bellard, M. D. Brice, B. A. Cartwright, A. Doubleday, H. Higgs, T. Hummelink, C. G. Hummelink-Peters, O. Kennard, W. D. S. Motherwell, J. R. Rodgers, D. G. Watson, *Acta Crystallogr., Sect. B* **1979**, *35*, 2331, and references therein; b) Inorganic Crystal Structure Data Base, National Institute of Standards and Technology, Fachinformationszentrum, Karlsruhe, Release 07/2.
[36] P. D'Angelo, G. Chillemi, V. Barone, G. Mancini, N. Sanna, I. Persson, *J. Phys. Chem. B* **2005**, *109*, 9178–9185.
[37] I. Persson, K. C. Dash, Y. Kinjo, *Acta Chem. Scand.* **1990**, *44*, 433–442.
[38] G. Schwarzenbach, H. Flaschka, *Die Komplexometrische Titration*, Ferdinand Enke, Stuttgart, **1965**, p. 212.
[39] CrysAlis Software system, Version 1.17, Xcalibur CCD System, Oxford Diffraction Ltd., **2003**.
[40] G. M. Sheldrick, SHELXS97 and SHELXL97, Computer Program for the Solution and Refinement of Crystal Structures, University of Göttingen, Göttingen (Germany), **1997**.
[41] A. L. Spek, *J. Appl. Crystallogr.* **2003**, *36*, 7–13.
[42] G. Bergerhoff, DIAMOND, Visual Crystal Structure Information System, Crystal Impact, K. Brandeburg & H. Putz GbR, Bonn (Germany), **1996**.
[43] A. Thompson, D. Attwood, E. Gullikson, M. Howells, K.-J. Kim, J. Kirz, J. Kortright, I. Lindau, P. Pianatta, A. Robinson, J. Scofield, J. Underwood, D. Vaughan, G. Williams, H. Winick, *X-ray Data Booklet*, LBNL/PUB-490 Rev. 2, Lawrence Berkeley National Laboratory, Berkeley, CA, **2001**.
[44] A. Filipponi, A. Di Cicco, C. R. Natoli, *Phys. Rev. B* **1995**, *52*, 15122–15134; A. Filipponi, A. Di Cicco, *Phys. Rev. B* **1995**, *52*, 15135–15149.
[45] E. D. Crozier, J. J. Rehr, R. Ingalls in *X-Ray Absorption, Principles, Applications, Techniques of EXAFS, SEXAFS, and XANES* (Eds.: D. C. Koningsberger, R. Prins), Wiley-Interscience, New York, **1988**, Chapter 9.
[46] S. I. Zabinsky, J. J. Rehr, A. Ankudinov, R. C. Albers, M. J. Eller, *Phys. Rev. B* **1995**, *52*, 2995–3009.
[47] P. D'Angelo, A. Di Nola, A. Filipponi, N. V. Pavel, D. Roccatano, *J. Chem. Phys.* **1994**, *100*, 985–994.
[48] A. Filipponi, *J. Phys. Condens. Matter* **1994**, *6*, 8415–8427.
[49] H. A. Levy, M. D. Danford, A. H. Narten, *Data Collection and Evaluation with an X-Ray Diffractometer Designed for the Study of Liquid Structure*, Report ORNL-3960, Oak Ridge National Laboratory, Oak Ridge, TN, **1966**.
[50] G. Johansson, M. Sandström, *Chem. Scr.* **1973**, *4*, 195–198.
[51] a) *International Tables for X-Ray Crystallography, Vol. A* (Ed.: T. Hahn), Kluwer, Dordrecht, **1995**; b) *International Tables for X-Ray Crystallography, Vol. C*, (Ed.: A. J. C. Wilson), Kynoch Press, Birmingham, **1974**.
[52] a) D. T. Cromer, *J. Chem. Phys.* **1969**, *50*, 4857–4859; b) D. T. Cromer, J. B. Mann, *J. Chem. Phys.* **1967**, *47*, 1892–1894.
[53] M. Molund, I. Persson, *Chem. Scr.* **1985**, *25*, 197–197.
[54] a) G. Johansson, *Adv. Inorg. Chem.* **1992**, *39*, 159–232, and references therein; b) T. Radnai, H. Ohtaki, *Chem. Rev.* **1993**, *93*, 1157–1204, and references therein.

Received: February 4, 2008
Published online: June 18, 2008

